

# RSC Advances



This is an *Accepted Manuscript*, which has been through the Royal Society of Chemistry peer review process and has been accepted for publication.

*Accepted Manuscripts* are published online shortly after acceptance, before technical editing, formatting and proof reading. Using this free service, authors can make their results available to the community, in citable form, before we publish the edited article. This *Accepted Manuscript* will be replaced by the edited, formatted and paginated article as soon as this is available.

You can find more information about *Accepted Manuscripts* in the [Information for Authors](#).

Please note that technical editing may introduce minor changes to the text and/or graphics, which may alter content. The journal's standard [Terms & Conditions](#) and the [Ethical guidelines](#) still apply. In no event shall the Royal Society of Chemistry be held responsible for any errors or omissions in this *Accepted Manuscript* or any consequences arising from the use of any information it contains.

SCHOLARONE™  
Manuscripts

RSC Advances Accepted Manuscript

# Preparation and characterization of flame retardant polyurethane foams containing phosphorus-nitrogen-functionalized lignin

Haibin Zhu,<sup>a</sup> Zumao Peng,<sup>a</sup> Yongmei Chen,<sup>a,\*</sup> Gaiyun Li,<sup>b</sup> Lei Wang,<sup>a</sup> Yang Tang,<sup>a</sup> Ran Pang,<sup>a</sup> Zia UL Haq Khan,<sup>a</sup> Pingyu Wan<sup>a,\*</sup>

## Abstract

Lignin, a natural macromolecule containing substantial aromatic rings and abundant hydroxyl groups, was firstly chemically grafted with phosphorus-nitrogen-containing groups via a liquefaction-esterification-salification process to prepare lignin-based phosphate melamine compound (LPMC). And then the LPMC which has remaining hydroxyl groups was used to substitute parts of polyols and copolymerize with isocyanate to produce lignin-modified-PU foam (PU-LPMC) with excellent flame retardancy. Owing to the rigid aromatic structure of lignin and the covalent linkages between LPMC and polymer-matrix, PU-LPMC showed nearly 2-fold increase in compression strength and excellent performance of thermal stability, char residue formation, self-extinguishment and inhibition from melt-dripping and smoke generation. Moreover, a large amount of non-flammable gases released during thermal degradation and a compact and dense intumescent (C-P-N-O)<sub>x</sub> char layer formed on the surface of the foams after combustion, resulting in the improvement of anti-flaming properties of the polymer by the flame retardancy of both gas phase and condensed phase.

**Keywords:** polyurethane foam, flame retardant, mechanical properties, lignin, phosphate, melamine

## 1. Introduction

Polyurethane (PU), an important class of thermoplastics, is prepared by polymerization of isocyanates with polyols. Owing to its low thermal conductivity, rigid PU foam is generally used as insulating material in construction, refrigeration, and piping/tubing industries.<sup>1</sup> However, the

inherently high flammability of PU has caused a large number of fire-related casualties and property losses in recent years.<sup>2,3</sup> Therefore, development of rigid PU foam with high mechanical strength (sufficient stiffness) and excellent fire-protection properties is urgently required.

Incorporation of flame-retardant (FR) additives into foams by simply mechanical mixing at the compounding stage is the most popular approach to improve the flame retardancy of PU.<sup>4</sup> Now halogenated flame-retardants have been abandoned because of environmental and safety problems.<sup>5-7</sup> The intumescent flame-retardant (IFR) containing phosphorus (as acid source) and nitrogen (as blowing agent) is considered to be effective and environmentally friendly.<sup>2, 8-10</sup> It reduces foam flammability by creating a fire-resistant charring layer on the materials to hinder heat and mass transfer between the gas and condensed phases.<sup>11-13</sup> However, IFRs (e.g. melamine polyphosphate) were usually physically added during polymerization and only a small addition (2 wt%) would cause serious deterioration (46%) in mechanical properties of the polymer due to its poor compatibility with polymers and the formation of localized stresses.<sup>13-15</sup>

In principle, an effective way of solving the contradiction between flame retardancy and mechanical strength is to link flame-retardants to the polymer-matrix through chemical covalent linkages. Lignin, a natural macromolecule with substantial aromatic structures and abundant hydroxyl groups,<sup>16,17</sup> is reported to be able to copolymerize with isocyanates by substituting parts of polyols to prepare PU. The results show that the mechanical strength of the obtained PU was improved because its rigid aromatic structure and high functionality of hydroxyl groups made lignin act as a toughening agent and thus improved the connectivity in the network of PU.<sup>18-20</sup> Although some researchers<sup>21</sup> believe that lignin has a certain degree of flame retardancy due to its aromatic structure helping to promote char formation, there is no evidence showing that directly adding lignin can significantly improve the flame retardancy of PU. Therefore, the flame retardancy has still been a big challenge until now. Based on this, we chose natural polymer lignin as the starting material, which was firstly chemically grafted with phosphorus-nitrogen-containing flame retardants to generate lignin-based phosphate melamine compound (LPMC), and then used to substitute parts of polyols and copolymerize with isocyanate through the remaining hydroxyl groups in LPMC to produce lignin-based-foams. As a result, the foams integrated with not only phosphorus and nitrogen but also plenty of aromatic structures. The former could account for the flame retarding ability, while the latter would offer good mechanical strength.

In the present paper, the preparation and structure characterization of phosphorus-nitrogen-functionalized lignin and the mechanical property, thermal stability and flame retardancy of the lignin-based PU material were studied systematically.

## 2. Experimental Section

### 2.1. Materials and chemicals

The crude lignin, derived from an enzymatic process of corn straw in ethanol production, was provided by Songyuan Chemical Co. Ltd. (China). Before using, lignin was purified according to the first procedure in our previous study.<sup>22, 23</sup> Firstly, lignin was dissolved in NaOH solution (pH=13) followed by centrifugation to remove the insolubles. The supernatant was then acidified with 10% hydrochloric acid to pH 2.0. After being heated at 80 °C for 10 min under stirring, lignin was precipitated and then filtered out after cooling down to room temperature. Then the solid was washed with dilute hydrochloric acid (pH=2.0) repeatedly for three times and rinsed with distilled water until neutral, and then dried and ground for further use.

Sodium lignosulfonate was purchased from Jiahe Wood Technology Co., Ltd. (Beijing, China). Polyethylene glycol (PEG-400, average molecular weight 400), glycerin, anhydrous aluminium chloride, polyphosphoric acid (PPA), ethylene glycol, and melamine were all analytical reagents and supplied by Beijing Chemical Plant (Beijing, China). Surfactant (Silicone-oil, AR) and catalyst (dibutyl tin dilaurate, AR) were purchased from Lingyunzhi Chemical Co., Ltd. (Xiamen, China) and Guangfu Fine Chemical Research Institute (Tianjin, China), respectively. Polyphenylmethane polyisocyanate (PMDI) was provided by Wanhua Chemical Group Co., Ltd. Water used in the study was deionized water (18 MΩ·cm).

### 2.2 Preparation of lignin-based phosphate melamine compound (LPMC)

The synthetic route for the lignin-based phosphate melamine compound (LPMC) from lignin contains three main steps: liquefaction, esterification and salification.

#### 2.2.1 Liquefaction

The purified lignin (6.00 g) and sodium lignosulfonate (1.80 g) were added to the mixed solvent of polyethylene glycol (PEG-400) (18.90 g) and glycerin (6.60g) in a 250ml three-neck flask. 0.67g

sulphuric acid ( $\text{H}_2\text{SO}_4$ , 98%) as the liquefaction catalyst was added under intense stirring. The flask was kept at 160 °C in an oil bath for 50 min while being constantly stirred, and the generated water was removed by nitrogen gas purge.

In order to characterize the liquefied-lignin, a small amount of liquefied products was collected and deionized water was added to precipitate lignin. The precipitate was then filtered out and washed with water repeatedly to remove the residual PEG-400 and glycerol. After drying, it was used for further analysis.

### 2.2.2 Esterification

1.66 g anhydrous aluminium chloride (5 wt% of total liquefied product) was added to the flask after liquefaction. The polyphosphoric acid (PPA) (19.98 g) was preheated at 80 °C for 5 min, and then poured into the flask. The reaction was kept at 160 °C under a steady stream of nitrogen gas and vigorous stirring for 4h. The generated water was removed by nitrogen gas purge.

### 2.2.3 Salification

4.50 g melamine was completely dissolved in 36 mL hot ethylene glycol, and then poured into the above flask. The reaction was kept at 160 °C under a steady stream of nitrogen gas for another 4 hours, then cooled down to room temperature followed by adding 100 mL deionized water. After vigorous stirring for 20 min, the solid product was totally precipitated and then filtered and washed with hot deionized water (70 °C) to remove the residues (PEG-400, glycerol, PPA and melamine), finally dried and ground into 200 mesh.

## 2.3 Preparation of lignin-modified-PU foams (PU-LPMC)

Different PU-LPMC samples were prepared as follows: blank 5.0 g PEG-400 and 5.0 g PEG-400 with 0.25g, 0.5g, 0.75g, 1.0g LPMC (corresponding to 5 %, 10 %, 15 % and 20 % of polyol) were added to 6 mL anhydrous dioxane in 5 beakers respectively, and kept at 70 °C under stirring for 10 min. After cooling down to room temperature, 0.75 g surfactant (silicone oil), 0.47 g catalyst (dibutyl tin dilaurate) and blowing agent (distilled water) were added to the 5 beakers respectively under stirring for 2 min, then 7.0 g, 7.5 g, 8.0 g, 9.0 g and 11.0 g of PMDI (corresponding to the same NCO/OH index) were added to the 5 beakers respectively with high speed agitation for 1min and then poured into 5 molds respectively to prepare free-rise foams. The solvent was removed in a vacuum oven at 80 °C for 24 h. Then each foam was shaped into different

sizes of sheets for further measurements. The obtained PU-LPMC composites with 5, 10, 15 and 20 wt% LPMC were designated as PU-LPMC<sub>5</sub>, PU-LPMC<sub>10</sub>, PU-LPMC<sub>15</sub> and PU-LPMC<sub>20</sub> respectively.

## 2.4 Characterization

The contents of phenolic hydroxyl groups were measured by potentiometric titration. The determination of total hydroxyl groups in lignin was performed by acetic anhydride acylation and potentiometric titration. Alcoholic hydroxyl contents were calculated by the difference between the total hydroxyl groups and the phenolic hydroxyl groups.<sup>22</sup> The available phosphorus content in LPMC was determined by quinoline phosphomolybdate gravimetric method (ISO 6598-1985 and GB/T 10512-2008), which is the total phosphorus content minus the water-soluble phosphorus content. Before phosphorus determination, the samples should be hydrolyzed by H<sub>2</sub>SO<sub>4</sub> (98%) / HNO<sub>3</sub> (65%) (volume ratio is 1:5) until colorless under heating. The contents of N element in LPMC were analyzed by a Vario EL cube Elemental Analyser instrument.

Fourier transform infrared spectroscopy (FT-IR) was applied with a Bruker Tensor 27 FT-IR spectrometer using KBr pellets. <sup>1</sup>H NMR and <sup>31</sup>P NMR spectra (400 MHz) were obtained at room temperature by a Bruker AV-400 NMR instrument with DMSO-d<sub>6</sub> as solvent, and tetramethylsilane (TMS) as the internal standard and H<sub>3</sub>PO<sub>4</sub> (85%) as the external standard respectively. The molecular weight distribution was determined by a Waters GPC 515-2410 System gel chromatography instrument with tetrahydrofuran as eluent at a flow rate of 1mL/min, and system calibration was performed with polystyrene standards.

The density of PU samples was measured according to ISO 845: 2006. The size of the specimen was no less than 100 cm<sup>3</sup>, and the average values of five samples were recorded. Determination of compression properties was performed with a Lloyd LR30K Plus universal material testing machine according to ISO 844: 2004 at a compressive speed of 5 mm min<sup>-1</sup>.

Thermal stability of LPMC and PU-LMPCs was characterized by thermogravimetry (TG) method on a thermal analyser (Netzsch 449 F3) in the range from 30 °C to 800 °C at a heating rate of 10 °C min<sup>-1</sup> in N<sub>2</sub> atmosphere. Char yields of the samples were determined with regard to the mass of the remaining residue at 800 °C. The gaseous products escaped during the thermal

degradation were identified on line by a FTIR spectrophotometer and a mass spectrometer (QMS403) coupled with the TG analyser (TG-TFIR-MS). The sample was heated from room temperature to 800 °C at a heating rate of 10 °C min<sup>-1</sup> in helium atmosphere with a gas flow rate of 50 mL min<sup>-1</sup>. The temperature of the connections for gas transportation between the apparatuses were set at 200 °C to allow the decomposition products in a gaseous state.

Scanning electron microscopy (SEM) was used to study morphological features on a Veeco DI scanning electron microscope under an accelerating voltage of 20 kV. A thin layer of gold was sprayed on the surface prior to SEM observation. The SEM-EDS-mapping was used to characterize the distributions of elements in the combustion residuals.

The limited oxygen index (LOI) values of PU-LPMC samples with dimension of 100 mm × 10 mm × 3 mm were measured on an NOSELAB-ATS EA04 oxygen index meter, according to standard test method GB/T 2406-2009. The UL-94 vertical test was carried out on a CZF3 vertical burning instrument (Jiangning Analysis Instrument Co., China) according to the UL 94 test standard. The specimens were 125 mm × 13 mm × 3 mm in dimension.

### 3. Results and discussion

#### 3.1 Characterization of LPMC

After the step of liquefaction, the chemical structure of liquefied-lignin was characterized. As shown in Table 1, the weight-average molecular weight ( $M_w$ ) of liquefied-lignin decreases significantly as compared with the raw material lignin, implying the linkages in lignin macromolecule were fractured during the liquefaction. In addition, the content of the phenolic hydroxyl groups in the liquefied-lignin slightly decreases (from original 1.63 mmol g<sup>-1</sup> to 1.43 mmol g<sup>-1</sup>) while the content of alcoholic hydroxyl groups increases obviously (from original 3.09 mmol g<sup>-1</sup> to 5.11 mmol g<sup>-1</sup>) as shown in Table 1. That is because some of the phenolic and alcoholic hydroxyl groups were etherified by glycerin and/or PEG and the excess hydroxyl groups brought by glycerin and/or PEG made the content of alcoholic hydroxyl groups in the liquefied-lignin increase. Furthermore, the FTIR spectra in Fig. 1 show that the ratio of the half band width of CH<sub>2</sub> groups (2933, 2875 and 1458 cm<sup>-1</sup>) or ether bonds (1110 cm<sup>-1</sup>) to that of the benzene ring (1512 cm<sup>-1</sup>) after liquefaction step (Fig. 1b) was increased compared to those in the original lignin (Fig. 1a).



Moreover, the peak around 3.2-3.8 ppm in  $^1\text{H}$  NMR (Fig. 2a, assigned to  $\text{CH}_2$  groups) increased after liquefaction step. All of the above results confirmed the introduction of glycerin (and/or PEG) and the formation of ether bond between glycerin (and/or PEG) and lignin during the liquefaction. This result is in agreement with the previous report.<sup>24</sup>

After liquefaction, esterification was carried out, during which some hydroxyl groups in the liquefied-lignin were consumed by the reaction with polyphosphoric acid, and then salification between melamine and the introduced phosphate groups was conducted, thus resulting in the formation of LPMC. Compared with the liquefied-lignin, the IR spectrum of LPMC in Fig. 1c shows that the new absorption peaks at  $1230\text{ cm}^{-1}$  (P=O stretching vibration),  $1056\text{ cm}^{-1}$  (O=P-O-C),<sup>25</sup>  $1149\text{ cm}^{-1}$  (P-O-P),  $1089\text{ cm}^{-1}$  (P-O-P), and  $980\text{ cm}^{-1}$  (P(=O)-OH)<sup>26-28</sup> indicate that phosphate groups were introduced into LPMC.  $^{31}\text{P}$  NMR (Fig. 2b) shows that phosphate groups in LPMC were bonded to both alcoholic ( $-9.8\text{ ppm}$ ,  $-\text{P}(=\text{O})-\text{O}_{\text{alco}}-\text{C}$ ) and phenolic ( $-13.4\text{ ppm}$ ,  $-\text{P}(=\text{O})-\text{O}_{\text{phen}}-\text{benzene}$ ) hydroxyl groups.<sup>29</sup> Moreover, the absorption peaks at  $3340$  and  $3136\text{ cm}^{-1}$  are assigned to the vibration of  $-\text{NH}_2$  and  $-\text{NH}_3^+$ , respectively.<sup>30,31</sup> The  $814\text{ cm}^{-1}$  peak attributed to the out of plane absorption of triazine rings in melamine shifts to a lower wavenumber,  $803\text{ cm}^{-1}$ , which was caused by the attachment of PPA on the molecules of melamine.<sup>32</sup> The above results proved that LPMC was fabricated successfully. By introducing P and N element in LPMC, the available P content in LPMC eventually is up to 13.1% and the N content is 16.8% (Table 1). The remaining alcoholic and phenolic hydroxyl groups in LPMC are 3.39 and 0.78 mmol/g respectively, such high contents are important for LPMC to substitute parts of polyols for crosslink with PMDI.

### 3.2 Cell morphology and mechanical properties of PU-LMPC

Although the color of PU-LPMC is much darker than PU (Fig. 3a), the homogeneity of the foam seems as good as PU. The SEM images of cross section for PU, PU-LPMC<sub>15</sub> and PU-LPMC<sub>20</sub> are shown in Fig. 3b-d. The shape of the cells in PU foam is approximately spherical as a whole, and no collapse is observed. Almost the same cell morphology is presented for PU-LPMC<sub>15</sub>, while the struts and strut joints are obviously thickened. As for the PU-LPMC<sub>20</sub>, the rupture of some struts and the collapse of cellular structure, even foam shrinkage are observed. This is because parts of

LPMC was not dissolved in the system when larger amounts of LPMC (20 wt%) were introduced, possibly making the poorly incorporated (dispersed) LPMC act as a cell-opening agent.

The density and mechanical properties of PU and PU-LPMC are summarized in Table 2. It is showed that the foam density increases with increasing amounts of LPMC, which is mainly due to the relatively high density of solid LPMC. It is noteworthy that the mechanical properties of the PU-LPMC, both Young's modulus and compression strength, are enhanced significantly as the substitution amount increases to 15%. Compared with pure PU foam, PU-LPMC<sub>15</sub> displays a nearly 2-fold increase in the compression stress and Young's modulus. However, the mechanical properties deteriorate obviously when the substitution amount of LPMC reaches 20% (but still better than PU foam), this is because the rigid benzene-ring structure in LPMC and the thickened struts and strut joints in foam enhanced the stiffness of PU-LPMC foam when the substitution amount of LPMC was less than 15%, while higher LPMC (more than 20 wt%) contents increased the frailability of PU-LPMC, which would induce the collapse of partial cellular structure as shown in SEM images.

### 3.3 Thermal behaviors of PU and PU-LPMC

Fig. 4 shows the TGA and DTG curves of the PU and PU-LPMCs, and the data are summarized in Table 3. The temperature at which 5 wt% of weight loss takes place is defined as the initial degradation temperature ( $T_{\text{initial}}$ ), and the temperature at which the degradation rate reaches a maximum is defined as  $T_{\text{max}}$ . Result shows that the  $T_{\text{initial}}$  of LPMC is 248 °C, and there are two  $T_{\text{max}}$  at 314°C and 383°C, which could be assigned to the scission of the phosphate ester bonds (230-350 °C) and the formation of intumescent char (360-520C) respectively.<sup>33</sup> Finally, the residue char of LPMC is 53.3% at 800 °C in N<sub>2</sub> atmosphere. Such a high residual weight implies LPMC is an excellent char-forming agent.

On the other hand, the  $T_{\text{initial}}$  of PU is 291 °C and there is only one  $T_{\text{max}}$  at 358 °C. With the help of TGA-FTIR/MS, large amount of combustible gas products except for H<sub>2</sub>O and CO<sub>2</sub>, such as 2-methyloxirane, CH<sub>2</sub>=CHOCH<sub>3</sub>, CH<sub>3</sub>CH<sub>3</sub>, C<sub>2</sub>H<sub>5</sub>OCH<sub>3</sub>, CH<sub>3</sub>OCH<sub>3</sub>, CH<sub>2</sub>=CHC<sub>2</sub>H<sub>5</sub> and CH<sub>2</sub>=CHCH<sub>3</sub>, were detected in the range of 290-450°C, while other gas products including *N*-methylaniline or *p*-methylaniline, aniline, ethylbenzene, toluene and benzene were detected at higher temperature (450-570 °C) (the FTIR spectra of gaseous pyrolysis products of PU in different

temperatures are shown in Fig. 5; Detailed confirmation of the degradation gas products is shown in Fig. S1, Fig. S2, Table S1 and Table S2 in the Supporting Information). Those small molecule products at lower temperature were assigned to the pyrolysis of the polyol soft segment in PU, and the products containing benzene ring came from pyrolysis of the PMDI hard segments in PU. Ultimately, only 14.6% of char was left above 600 °C, indicating pure PU was an inflammable material.

The  $T_{\text{initial}}$  of the PU-LPMC foams is slightly lower than that of pure PU sample since LPMC degrades easier than PU, which was necessary for intumescent flame-retardant systems because flame retardants had to be degraded earlier to accelerate the carbonization of polymer-matrix.<sup>33</sup> Moreover, both  $T_{\text{max1}}$  and  $T_{\text{max2}}$  for PU-LPMC are higher than the only one  $T_{\text{max}}$  for PU. It is noteworthy that the weight loss of PU-LPMC shifted gradually from low temperature (first degradation stage) to high temperature (second degradation stage) with increasing LPMC content, implying the enhancing effect on thermal stability by LPMC. During the thermal degradation of PU-LPMC<sub>15</sub>, plenty of non-flammable gas products such as H<sub>2</sub>O, CO<sub>2</sub>, NH<sub>3</sub> and only a small amount of CH≡CH, CH<sub>3</sub>CH<sub>3</sub> and CH<sub>3</sub>CH<sub>2</sub>NH<sub>2</sub> or CH<sub>3</sub>NHCH<sub>3</sub> were detected (the FTIR spectra of gaseous pyrolysis products of PU-LPMC<sub>15</sub> are shown in Fig. 6; Detailed confirmation is shown in the Supporting Information). These non-flammable gases could dilute the oxygen concentration in the air around the burning polymer, slowing down the flame propagation. In addition, more residual char formed for PU-LPMC than for PU, and the amount increased greatly with increasing the LPMC content. Assuming no effect of LPMC on the formation of residual char, the “theoretical” char residues of PU-LPMC<sub>5</sub>, PU-LPMC<sub>10</sub>, PU-LPMC<sub>15</sub> and PU-LPMC<sub>20</sub> could be calculated based on the amount of both the components in PU-LPMC, but the results (list in Table 3) show that the actual char residues are higher than the calculated values. That proves the phosphorus and nitrogen in LPMC contributed to the dehydration of polymer to form char. Enhancement of the char formation was beneficial to limitation of the generating combustible gases, decrease in exothermicity of pyrolysis reaction, and reduction of thermal conductivity of the burning material, thus lowering flammability of the material.

### 3.4 Flame retardancy of PU-LPMC

The limited oxygen index (LOI) is the minimum oxygen concentration (vol%) which would support the combustion of a certain material, so the higher LOI value represents the better flame retardancy.<sup>34</sup> In Table 4, the results show that the LOI values of PU-LPMCs increase with increasing LPMC contents, indicating the enhancing effect on flame retardancy by LPMC. In detail, the combustion processes of PU and PU-LPMC<sub>15</sub> are illustrated in Fig. 7. For pure PU, when the testing oxygen concentration was 19.2 vol%, the sample was ignited quickly with rapid flame propagation and a great deal of thick smoke was generated during the combustion process. Meanwhile, melt-dripping with fire could be observed after burning for 40 seconds and serious bending deformation of the material was seen after 60 seconds burning. However, for the PU-LPMC<sub>15</sub> tested at an oxygen concentration of 26.7 vol%, when the sample was ignited, flame propagation apparently slowed down; then the flame gradually became smaller, and finally extinguished within 49 seconds. Moreover, it was obvious that the smoke reduced significantly during combustion and the PU-LPMC composite still maintained its original shape.

The UL-94 vertical burning test is another common method that ranks the flammability of materials. As shown in Table 4, the pure PU foam was highly combustible and failed to pass the UL-94 test, but PU-LPMCs showed better performance in the UL-94 test. Small substitution amount of LPMC (PU-LPMC<sub>5</sub>) could eliminate the phenomenon of melt dripping and the V-1 rate could be achieved for PU-LPMC<sub>15</sub> foam, revealing an important role of LPMC in restraining the inflammation.

Fig. 8 shows the digital photographs of combustion residues and the inner morphology of PU and PU-LPMC<sub>15</sub> samples after combustion test. Only char was left over after PU was burned out, however, there were still some unburned parts remaining under the residual char of PU-LPMC, implying the excellent flame retardancy of LPMC. Interestingly, an intumescent char layer was formed on the surface of PU-LPMC composite, which was considered to play an important role in flame retardancy.

### 3.5 Morphological characterization of the char residues

To further elucidate the anti-flaming performance of the intumescent char layer, the morphology and elemental analysis of the char residue were characterized by SEM-EDS. Fig. 9 shows the microstructures of outer and inner char of PU and PU-LPMC<sub>15</sub> formed in the combustion

test. It is observed in Fig. 9a, a' and a'' that there are numbers of holes (40-100 $\mu\text{m}$ ) on the outer char of PU, and its inner char is loose and permeable. Therefore, they could not provide a good flame shield for the underlying polymeric substrate. In contrast, as shown in Fig. 9b, b' and b'', both the outer and inner char of PU-LPMC are much more continuous and compact. Moreover, the outer surface has plenty of rugged creases, while a large number of bubbles (10-30 $\mu\text{m}$ ) pack together closely on the inner surface. This intumescent char layer could slow down heat and mass transfer between gas and the condensed phases, and prevents the underlying polymeric substrate from further attack by heat flux.

By the elemental mapping technique of SEM-EDS, the spatial distributions of O, P and N elements in PU-LPMC<sub>15</sub> combustion residues (outer surface) could be clearly observed. As shown in Fig. 10a-d, the elements of P and N still remain in the final chars after combustion and reveal a uniform distribution. Meanwhile, the phosphorus remaining in the char residue tested by the quinoline phosphomolybdate gravimetric method is 5.13%, showing higher than the original phosphorus content in the PU-LPMC<sub>15</sub> (the value is 1.96%). This may be the result of promoting dehydration and carbonization of PU by LPMC during combustion and forming a compact (C-P-N-O)<sub>x</sub> composite layer as a good flame shield to protect the underlying material.

#### 4. Conclusions

LPMC was successfully prepared by grafting phosphorus-nitrogen-containing groups on lignin via a three-step reaction and then used to substitute parts of polyols to produce flame retardant PU foam composite based on its remaining hydroxyl groups. The addition of LPMC exhibited negligible negative influence on the morphology and mechanical properties of PU when the substitution amount did not exceed 15 wt %. Excess LPMC content would lead to the collapse of cell structure and the rupture of cell walls. Compared to pure PU, PU-LPMC<sub>15</sub> displayed a nearly 2-fold increase in compressive strength and excellent performance of thermal stability, char residue formation, self-extinguishment and inhibition from melt-dripping and smoke generation. In addition, LPMC could promote the generation of non-flammable gases during PU degradation, inhibiting the flame propagation and dehydration of PU to form a compact (C-P-N-O)<sub>x</sub> char layer shielding the underlying polymeric substrate from further attack by heat flux, thus endowing PU with excellent

flame retardancy. This flame-retarded functionalized-lignin provided a promising alternative for environmentally friendly (no need for toxic chemicals) and value-added utilization of the abandoned lignin and sustainable supply of raw materials for flame retardant PU production. Importantly, this functionalized-lignin could also be used in other fields, such as flame retardant of epoxy resin and polypropylene materials.

## Acknowledgements

The authors greatly appreciate the support from the national natural science foundation of China (No. 51374016) and Chinese universities scientific Fund (No. JD1313). The authors thank Prof. Xiaoguang Liu and Prof. Sheng Zhang for valuable suggestions in the preparation of this manuscript.

## Notes and references

<sup>a</sup> National Fundamental Research Laboratory of New Hazardous Chemicals Assessment and Accident Analysis, Beijing Key Laboratory of Environmentally Harmful Chemical Analysis, Beijing University of Chemical Technology, 100029 Beijing, China

<sup>b</sup> Key Laboratory of Wood Science and Technology of SFA, Research Institute of Wood Industry, Chinese Academy of Forestry, Beijing 100091, China

\*Corresponding Authors: E-mail: [chenym@mail.buct.edu.cn](mailto:chenym@mail.buct.edu.cn);

E-mail: [pywan@mail.buct.edu.cn](mailto:pywan@mail.buct.edu.cn)

† Electronic supplementary information (ESI) available: See DOI: 10.1039/b000000x/

1. H. W. Engels, H. G. Pirkl, R. Albers, R. W. Albach, J. Krause, A. Hoffmann, H. Casselmann and J. Dormish, *Angew. Chem. Int. Edit.*, 2013, **52**, 9422-9441.
2. S. Bourbigot and S. Duquesne, *J. Mater. Chem.*, 2007, **17**, 2283-2300.
3. Y. S. Kim, Y. C. Li, W. M. Pitts, M. Werrel and R. D. Davis, *ACS Appl. Mater. Inter.*, 2014, **6**, 2146-2152.
4. H. Singh and A. K. Jain, *J. Appl. Polym. Sci.*, 2009, **111**, 1115-1143.

5. R. C. Hale, S. L. Kim, E. Harvey, M. J. La Guardia, T. M. Mainor, E. O. Bush and E. M. Jacobs, *Environ. Sci. Technol.*, 2008, **42**, 1452-1457.
6. R. C. Hale, M. J. La Guardia, E. P. Harvey, M. O. Gaylor, T. M. Mainor and W. H. Duff, *Nature*, 2001, **412**, 140-141.
7. A. Blum, *Science*, 2007, **318**, 194-196.
8. S. Y. Lu and I. Hamerton, *Prog. Polym. Sci.*, 2002, **27**, 1661-1712.
9. H. Y. Ma, L. F. Tong, Z. B. Xu and Z. P. Fang, *Adv. Funct. Mater.*, 2008, **18**, 414-421.
10. Y. C. Li, S. Mannen, A. B. Morgan, S. C. Chang, Y. H. Yang, B. Condon and J. C. Grunlan, *Adv. Mater.*, 2011, **23**, 3926-3931.
11. S. Jahromi, W. Gabrielse and A. Braam, *Polymer*, 2003, **44**, 25-37.
12. J. W. Gu, G. C. Zhang, S. L. Dong, Q. Y. Zhang and J. Kong, *Surf. Coat. Technol.*, 2007, **201**, 7835-7841.
13. M. Thirumal, D. Khastgir, G. B. Nando, Y. P. Naik and N. K. Singha, *Polym. Degrad. Stabil.*, 2010, **95**, 1138-1145.
14. S. V. Levchik and E. D. Weil, *J. Fire Sci.*, 2006, **24**, 345-364.
15. P. A. Song, Y. Shen, B. X. Du, M. Peng, L. Shen and Z. P. Fang, *ACS Appl. Mater. Inter.*, 2009, **1**, 452-459.
16. A. J. Ragauskas, C. K. Williams, B. H. Davison, G. Britovsek, J. Cairney, C. A. Eckert, W. J. Frederick, J. P. Hallett, D. J. Leak, C. L. Liotta, J. R. Mielenz, R. Murphy, R. Templer and T. Tschaplinski, *Science*, 2006, **311**, 484-489.
17. J. Zakzeski, P. C. A. Bruijninx, A. L. Jongerius and B. M. Weckhuysen, *Chem. Rev.*, 2010, **110**, 3552-3599.
18. Y. Li and A. J. Ragauskas, *J. Wood. Chem. Technol.*, 2012, **32**, 210-224.
19. Y. Li and A. J. Ragauskas, *RSC Adv.*, 2012, **2**, 3347-3351.
20. S. J. Hu, C. X. Wan and Y. B. Li, *Bioresour. Technol.*, 2012, **103**, 227-233.
21. A. De Chirico, M. Armanini, P. Chini, G. Cioccolo, F. Provasoli and G. Audisio, *Polym. Degrad. Stabil.*, 2003, **79**, 139-145.
22. H. B. Zhu, Y. M. Chen, T. F. Qin, L. Wang, Y. Tang, Y. Z. Sun and P. Y. Wan, *RSC Adv.*, 2014, **4**, 6232-6238.

23. H. B. Zhu, L. Wang, Y. M. Chen, G. Y. Li, H. Li, Y. Tang and P. Y. Wan, *RSC Adv.*, 2014, **4**, 29917-29924.
24. E. Jasiukaityte, M. Kunaver and C. Crestini, *Catal. Today*, 2010, **156**, 23-30.
25. P. Lv, Z. Z. Wang, K. L. Hu and W. C. Fan, *Polym. Degrad. Stabil.*, 2005, **90**, 523-534.
26. S. V. Levchik, G. Camino, L. Costa and G. F. Levchik, *Fire. Mater.*, 1995, **19**, 1-10.
27. A. I. Balabanovich, *Thermochim. Acta*, 2005, **435**, 188-196.
28. Y. Liu and Q. Wang, *Polym. Degrad. Stabil.*, 2006, **91**, 2513-2519.
29. O. Kühl, Springer-Verlag, Berlin, Heidelberg, 2008; Chapter 4, pp 31-35.
30. M. J. Chen, Z. B. Shao, X. L. Wang, L. Chen and Y. Z. Wang, *Ind. Eng. Chem. Res.*, 2012, **51**, 9769-9776.
31. Y. H. Chen and Q. Wang, *Polym. Degrad. Stabil.*, 2006, **91**, 2003-2013.
32. Z. Z. Wang, P. Lv, Y. Hu and K. L. Hu, *J. Anal. Appl. Pyrol.*, 2009, **86**, 207-214.
33. H. Y. Ma, L. F. Tong, Z. B. Xu, Z. P. Fang, Y. M. Jin and F. Z. Lu, *Polym. Degrad. Stabil.*, 2007, **92**, 720-726.
34. X. D. Qian, L. Song, B. Yu, B. B. Wang, B. H. Yuan, Y. Q. Shi, Y. Hu and R. K. K. Yuen, *J. Mater. Chem. A*, 2013, **1**, 6822-6830.



## List of Tables and Figures

**Table 1** Hydroxyl contents, molecular weight distribution, and the content of elements of P and N of all samples

**Table 2** Mechanical properties and densities of PU with and without LPMC

**Table 3** Data of TGA and DTG for various samples at a heating rate of  $10\text{ }^{\circ}\text{C min}^{-1}$  in  $\text{N}_2$ .

**Table 4** Results from LOI and UL-94 measurements for PU with and without LPMC.

**Fig. 1** The FTIR spectra of lignin (a), liquefied-lignin (b), and LPMC (c)

**Fig. 2** The  $^1\text{H}$  NMR spectra of lignin and liquefied-lignin (a) and  $^{31}\text{P}$  NMR spectra of lignin-based phosphate (b)

**Fig. 3** The digital photograph of the synthesized polyurethane foam with (right) and without (left) LPMC (a); scanning electron microscopy (SEM) photographs of the surface of PU (b), PU-LPMC<sub>15</sub> (c), and PU-LPMC<sub>20</sub> (d).

**Fig. 4** TGA (a) and DTG (b) curves for PU and PU-LPMC.

**Fig. 5** FTIR spectra of the gaseous pyrolysis products of PU in different temperatures.

**Fig. 6** FTIR spectra of the gaseous pyrolysis products of PU-LPMC<sub>15</sub> in different temperatures.

**Fig. 7** Combustion processes of PU and PU-LPMC<sub>15</sub> at oxygen concentrations of 19.2 and 26.7 vol%, respectively.

**Fig. 8** The digital photographs of combustion residues and the inner morphology of PU (a) and PU-LPMC<sub>15</sub> (b) samples after combustion test.

**Fig. 9** SEM micrographs of the char formed after combustion: outer (a) and inner (a' and a'') char of sample PU; outer (b) and inner (b' and b'') char of sample PU-LPMC<sub>15</sub>.

**Fig. 10** SEM micrographs of the char in PU-LPMC<sub>15</sub> formed after combustion (a); SEM-EDS-mapping of O (b), N (c) and P (d) elements in the char of PU-LPMC<sub>15</sub> after combustion.

**Table 1** Hydroxyl contents, molecular weight distribution, and the content of elements of P and N of all samples

	Hydroxyl contents		Molecular weight			Element content	
	<sup>a</sup> OH <sub>alco</sub> (mmol g <sup>-1</sup> )	<sup>b</sup> OH <sub>phen</sub> (mmol g <sup>-1</sup> )	M <sub>w</sub>	M <sub>n</sub>	Polydispersity (M <sub>w</sub> / M <sub>n</sub> )	P (%)	N (%)
Lignin	3.09	1.63	3021	858	3.521	—	—
Liquefied-lignin	5.11	1.43	1411	728	1.938	—	—
LPMC	3.39	0.78	—	—	—	13.1	16.8

<sup>a</sup> OH<sub>alco</sub> : alcoholic hydroxyl group.      <sup>b</sup> OH<sub>phen</sub> : phenolic hydroxyl group.

**Table 2** Mechanical properties and densities of PU with and without LPMC

sample	LPMC content (%)	Density (g cm <sup>-3</sup> )	Compression stress at Limit (MPa)	Young's Modulus (MPa)
1	0	0.184	0.51 ± 0.03	11.34 ± 0.23
2	5	0.222	0.99 ± 0.02	20.46 ± 0.08
3	10	0.236	1.28 ± 0.01	29.82 ± 0.08
4	15	0.245	1.46 ± 0.04	31.56 ± 0.12
5	20	0.267	0.89 ± 0.02	18.84 ± 0.14

**Table 3** Data of TGA and DTG for various samples at a heating rate of 10 °C min<sup>-1</sup> in N<sub>2</sub>

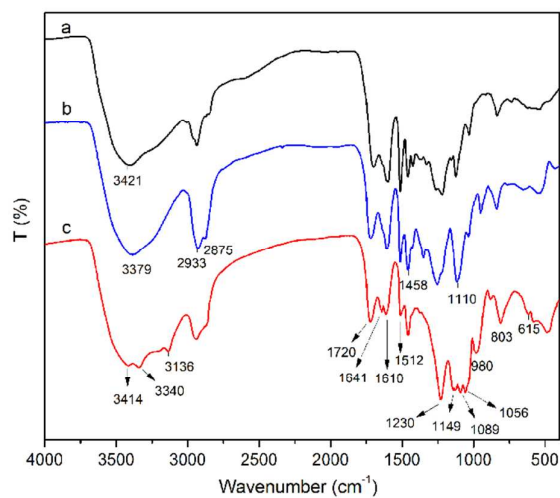
sample	<sup>a</sup> T <sub>initial</sub> (°C)	<sup>b</sup> T <sub>max</sub> (°C)		Residue at 800 °C (wt%)	Theoretical residual
		1st stage	2nd stage		
LPMC	248.1	314.3	383.2	53.3	—
PU	291.0	358.2	—	14.6	—
PU-LPMC <sub>5</sub>	287.6	358.7	406.1	17.2	16.5
PU-LPMC <sub>10</sub>	283.6	359.2	407.4	22.2	18.4
PU-LPMC <sub>15</sub>	282.2	359.6	408.2	24.4	20.4
PU-LPMC <sub>20</sub>	282.0	360.1	408.5	27.7	22.3

<sup>a</sup> T<sub>initial</sub>: initial degradation temperature (temperature at 5% weight loss).  
<sup>b</sup> T<sub>max</sub>: maximum weight loss temperature.

**Table 4** Results from LOI and UL-94 measurements for PU with and without LPMC

	LOI (%)	UL-94 rating	
		UL-94 rating	Dripping
PU	18.9	<sup>a</sup> NC	Y
PU-LPMC <sub>5</sub>	23.4	NC	N
PU-LPMC <sub>10</sub>	24.8	NC	N
PU-LPMC <sub>15</sub>	26.7	V-1	N
PU-LPMC <sub>20</sub>	28.3	V-1	N

<sup>a</sup> NC: no classification.

**Fig. 1** The FTIR spectra of lignin (a), liquefied-lignin (b), and LPMC (c)

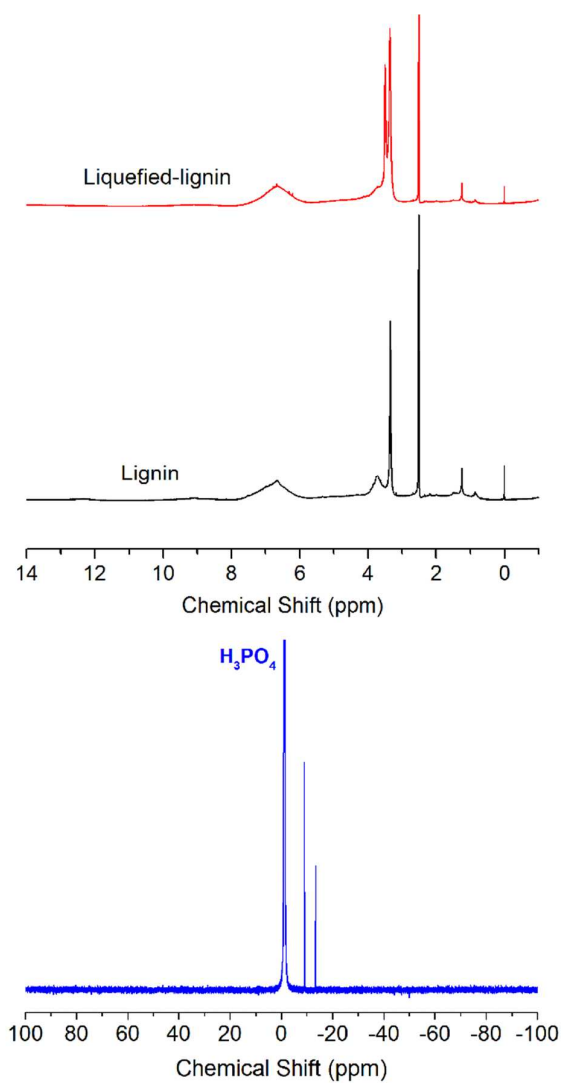


**Fig. 2** The  $^1\text{H}$  NMR spectra of lignin and liquefied-lignin (a) and  $^{31}\text{P}$  NMR spectra of lignin-based phosphate (b)

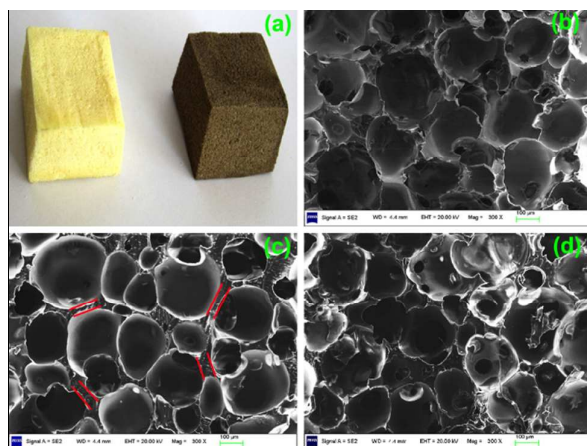


**Fig. 3** The digital photograph of the synthesized polyurethane foam with (right) and without (left) LPMC (a); scanning electron microscopy (SEM) photographs of the surface of PU (b), PU-LPMC<sub>15</sub> (c), and PU-LPMC<sub>20</sub> (d).

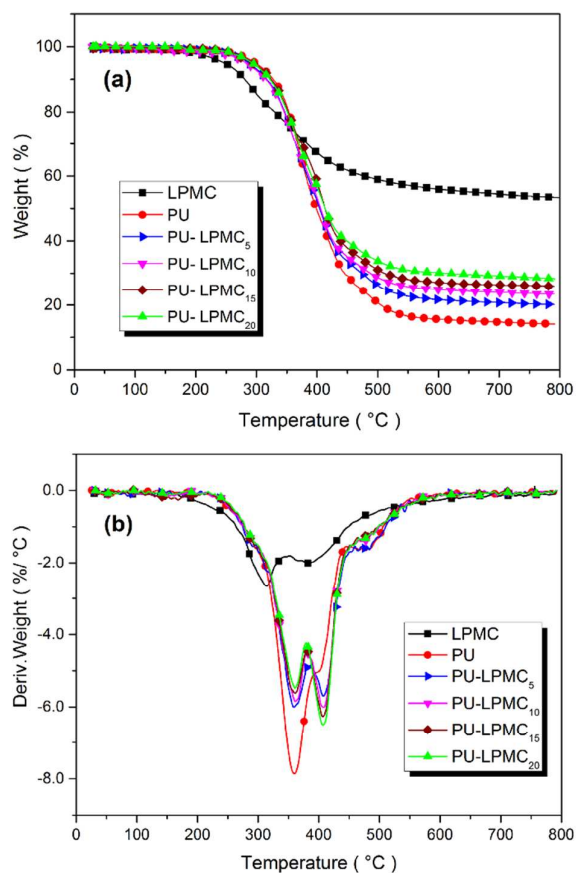


**Fig. 4** TGA (a) and DTG (b) curves for PU and PU-LPMC.

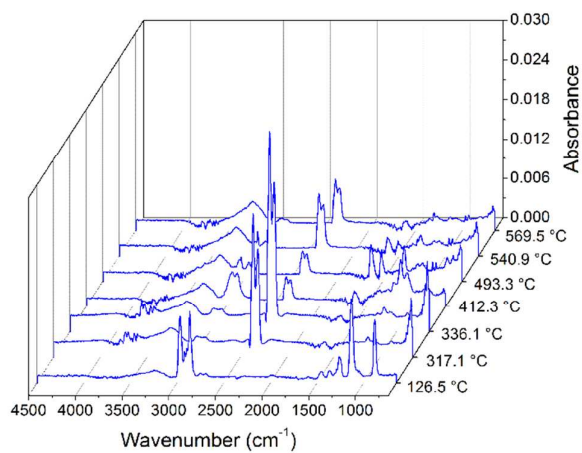


**Fig. 5** FTIR spectra of the gaseous pyrolysis products of PU in different temperatures.

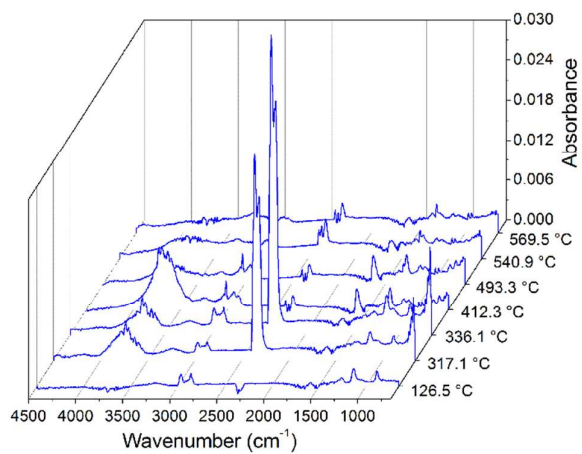


**Fig. 6** FTIR spectra of the gaseous pyrolysis products of PU-LPMC<sub>15</sub> in different temperatures.

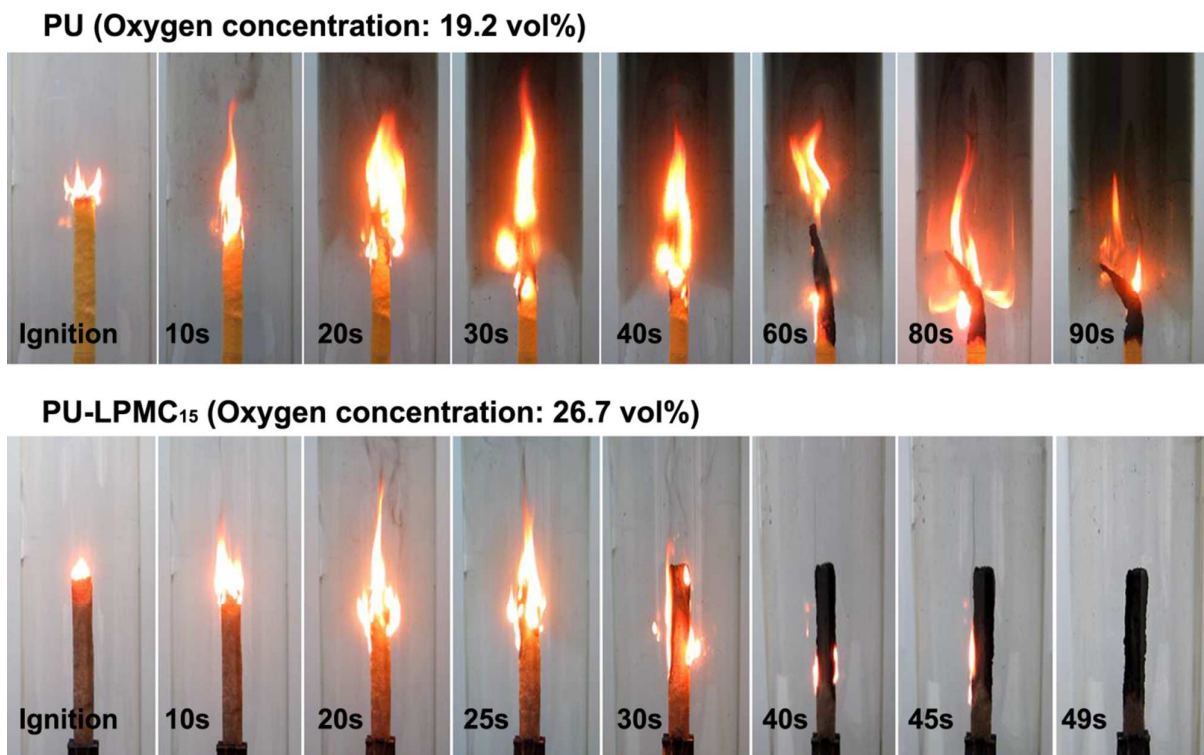


**Fig. 7** Combustion processes of PU and PU-LPMC<sub>15</sub> at oxygen concentrations of 19.2 and 26.7 vol%, respectively.

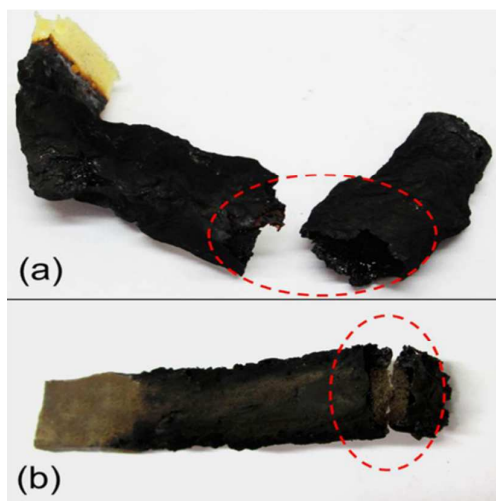


**Fig. 8** The digital photographs of combustion residues and the inner morphology of PU (a) and PU-LPMC<sub>15</sub> (b) samples after combustion test.

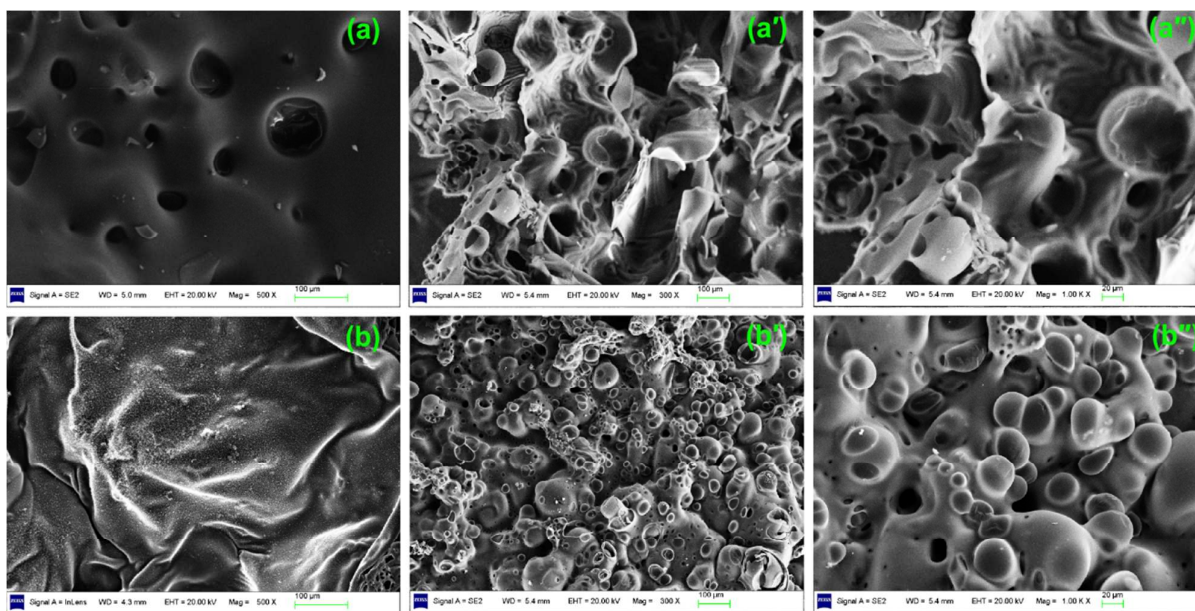


**Fig. 9** SEM micrographs of the char formed after combustion: outer (a) and inner (a' and a'') char of sample PU; outer (b) and inner (b' and b'') char of sample PU-LPMC<sub>15</sub>.

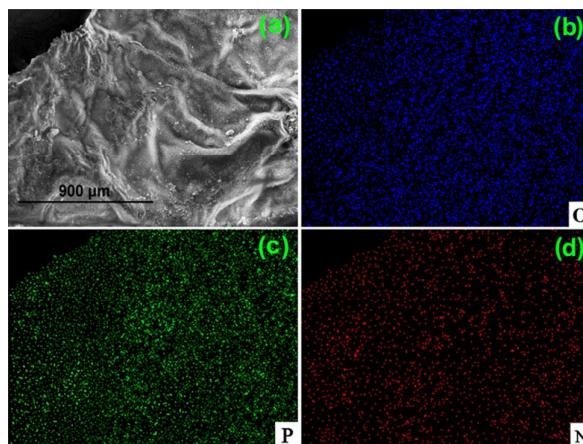


**Fig. 10** SEM micrographs of the char in PU-LPMC<sub>15</sub> formed after combustion (a); SEM-EDS-mapping of O (b), N (c) and P (d) elements in the char of PU-LPMC<sub>15</sub> after combustion.



